

Justification of the effective fractional Coulomb energy and the extended Brinkman-Rice picture *

Hyun-Tak Kim **

Telecom. Basic Research Lab., ETRI, Taejon 305-350, Korea

In order to calculate the effective mass of quasiparticles for a strongly correlated metallic system in which the number of carriers, n , is less than that of atoms (or lattices), l , the metallic system is averaged by one effective charge per atom over all atomic sites. The effective charge of carriers, $\langle e \rangle = (n/l)e = \rho e$, and the on-site effective Coulomb repulsion, $U = \rho^2 \langle \frac{e^2}{r} \rangle \equiv \rho^2 \kappa U_c$, are defined and justified by means of measurement. ρ is band filling and κ is the correlation strength. The effective mass, $\frac{m^*}{m} = \frac{1}{1 - \kappa^2 \rho^4}$, calculated by the Gutzwiller variational theory, is regarded as the average of the true effective mass in the Brinkman-Rice (BR) picture and is the effect of measurement. The true effective mass has the same value irrespective of ρ , and is not measured experimentally. The true correlation strength of the BR picture is evaluated as $0.90 < \kappa_{BR} < 1$ for $\text{Sr}_{1-x}\text{La}_x\text{TiO}_3$ and $0.92 < \kappa_{BR} < 1$ for YBCO. High- T_c superconductivity for YBCO is attributed to the true effective mass caused by the large κ_{BR} value. The effective mass explains the metal-insulator transition of the first order on band filling. Furthermore, the pseudogap is predicted in this system.

I. INTRODUCTION

Ever since a correlation-driven metal-Mott-insulator transition¹ of the first order (called the "Mott transition") was predicted in 1949, the Mott transition has never been completely solved. The Hubbard model², one of the theories explaining the Mott transition, showed the second-order metal-insulator transition (MIT) by increasing the on-site Coulomb repulsion U , whereas the Brinkman-Rice (BR) picture³, based on Gutzwiller's variational theory⁴, explained the first-order transition at $U/U_c=1$ for the first time. The infinite dimensional ($d = \infty$) Hubbard model suggested that the MIT occurs while going from U/W to U_c/W , and that the metallic side exhibits the BR picture.⁵ Here W is the band width. The $d = \infty$ Hubbard model and the BR picture were built on a metallic system with an electronic structure of one electron per atom. However the metallic system which Gutzwiller assumed is a general one without limiting the number of electrons per atom. Furthermore, observations and current understanding of the MIT driven by correlation effects were reviewed.^{6,7} Validity of the BR picture and the Mott transition was also discussed by theorists, which is because the BR picture has not been proved experimentally.^{8,9}

Experimentally, for the coefficient γ of the heat capacity of $\text{Sr}_{1-x}\text{La}_x\text{TiO}_3$ (SLTO) which is proportional to the effective mass, the sharp first-order transition was observed between $x=0.95$ and 1.^{10,11} This transition was regarded as the Mott transition on band filling, which could not be explained by the above mentioned Hubbard models and the BR picture. This is because the structure of the metallic system of SLTO is not one electron per atom. Hence, when the number of carriers is less than the number of atoms, the MIT of first-order on band filling has remained a theoretical problem. In particular, the metallic property near the Mott transition is still controversial.¹²⁻¹⁴ Furthermore the effective mass of

quasiparticles as a function of band filling is necessary to take account of high T_c superconductivity.¹⁵

Recently, an insight on both the effective mass and the Mott transition was proposed on the basis of $U = \rho^2 \langle \frac{e^2}{r} \rangle$ and experimental data.¹⁶ However the justification of $U = \rho^2 \langle \frac{e^2}{r} \rangle$ and exact calculations for the effective mass were not given. Thus the problem of the Mott transition on band filling remains unanswered.

In this paper, when the number of carriers is less than the number of atoms, the necessity of the development of $\langle e \rangle = \rho e$ is given by introducing the instability of the charge-density-wave potential energy, and the justification of $\langle e \rangle = \rho e$ and $U = \rho^2 \langle \frac{e^2}{r} \rangle$ is given by means of measurement. The effective mass of quasiparticles is exactly calculated on the basis of the Gutzwiller variational theory. Furthermore, true correlation strengths of the BR picture, not given in reference 16, are evaluated for $\text{Sr}_{1-x}\text{La}_x\text{TiO}_3$ and YBCO.

II. EFFECTIVE FRACTIONAL COULOMB ENERGY

A strongly correlated metallic system of the s band structure is assumed for a $d = \infty$ dimensional simple-cubic lattice. Let n and l be the number of electrons (or carriers) and the number of atoms (or lattices), respectively. In the case of one electron per atom, *i.e.*, $n = l$, the metallic system is a metal and the existence probability ($P = n/l = \rho =$ band filling) of electrons on nearest-neighbor sites is one. The on-site Coulomb repulsion is always given by $U = U' \equiv \langle \frac{e^2}{r} \rangle$ and an electron on an atom has a spin, as shown in Fig. 1 (a). However, in the case of $n < l$ by doping an element to a base insulator or metal, U is determined by probability. The metallic system is quite complicated, as shown in Fig. 1 (b). Four types of regions for the system can be distinguished as possible extreme examples. Region A in Fig. 1 (b) has no electrons

on its atomic sites, which corresponds to a normal insulator. Region C has the metallic structure of one electron per atom. Regions B and D have a charge-density-wave (CDW) structure unlike the assumed cubic. This must be regarded as a CDW insulator with the CDW-energy gap¹⁷ depending on the local CDW-potential energy.^{17,18} Moreover, even when one electron on an atom is removed in Fig. 1 (a), both nearest-neighbor sites of the atom without an electron and the atom itself also are regarded as region B. The CDW-potential energy is defined by $V_{CDW} = -E_p(Q_i - Q_j)^2$, where Q_i and Q_j are charges irrespective of spins on i and j sites, respectively. E_p is the small-polaron binding energy which is a constant of electron-phonon coupling. The potential energy is derived by breathing-mode distortion (or frozen-breathing mode) due to a charge disproportionation ($\delta Q = Q_i - Q_j$) between nearest-neighbor sites. The CDW-energy gap is regarded as a pseudogap (or pinned CDW gap) for this system. Here δQ is called the electronic structure factor in real-space. $\delta Q=0$ indicates that the electronic structure is metallic, while $\delta Q \neq 0$ suggests that it is insulating. In addition, V_{CDW} can also be expressed in terms of band filling as follows: $V_{CDW} = -E_p(1 - \rho)^2 = -E_p\mu^2$, where $\mu = 1 - \rho = n_b/l$ (or $n_b = l - n$), n_b is the number of bound charges bounded by V_{CDW} .¹⁸ As ρ increases, μ decreases. This indicates that the pseudogap in the CDW insulating phase decreases as the metallic phase increases, because the pseudogap depends upon V_{CDW} .

Conversely, the pseudogap, as observed by optical methods,¹⁹⁻²² photoemission spectroscopy,²³ and heat capacity measurement^{24,25} for high- T_c superconductors, necessarily occurs if the number of carriers is less than the number of atoms. Therefore, the metallic system is inhomogeneous and cannot be self-consistently represented in k -space, *i.e.*, U and the density of states of the system are not given. Thus, in order to overcome this difficulty, charges on atoms in the metal phase (region C) have to be averaged over sites, as shown in Fig. 1 (c). The on-site effective charge is $Q_i = Q_j = \langle e \rangle = (n/l)e = \rho e$, on average over sites. The metallic system, then, is a metal, because $V_{CDW} = 0$ due to $\delta Q=0$. This system is analogous to the case of one electron per atom, such as Fig. 1 (a). Therefore, the effective Coulomb energy is given by $U = \rho^2 U'$, as shown in Fig. 1 (c).

To illustrate the physical meaning of $P = \langle e \rangle / e = \rho < 1$, then $\mu \ll 1$, $\rho = 1 - \mu < 1$. For the CDW insulating side, $\mu \ll 1$ indicates that there are a few doubly occupied atoms such as in region D, while, for the metallic side, $\rho < 1$ indicates that a number of carriers exist. In other words, this suggests that region C is extremely wide.

The insulating and metallic sides correspond to two phases, which are attributed to the metal-insulator instability (or instability of the CDW-potential energy)¹⁸ at $\rho=1$ (half filling). This indicates that metals with the electronic structure of Fig. 1 (a) are not synthesized. Junod et al.²⁶ suggested that even the best samples are not 100% superconducting, which supports the metal-

insulator instability¹⁸. Thus synthetic metals composed of several atoms always have the electronic structure of two phases such as Fig. 1 (b), which is a necessity of the development of $\langle e \rangle = \rho e$.

To justify the fractional charge of carriers of the metallic system with two phases, the concept of measurement is necessary. In the case of measuring charge of carriers in the metallic system of Fig. 1 (b), the measured charge becomes the effective fractional one, $\langle e \rangle = \rho e$, with the average meaning of the system because experimental data for the metallic system are expectation values of statistical averages. In the case of not measuring charge, the charge of carriers in region C in Fig. 1 (b) remains the true elementary one not observed by means of measurement.

Accordingly, for the metallic system of the $n \leq l$ case, the effective fractional Coulomb energy, $U = \rho^2 U'$, is defined by using $\langle e \rangle = \rho e$ and justified by means of measurement.

Furthermore, $U = \rho^2 U'$, deduced on the basis of the CDW concept, can be applied to even cuprate systems such as $\text{La}_{1-x}\text{Sr}_x\text{Cu}_2\text{O}_4$ (LSCO). This is because the MIT with x from the antiferromagnetic insulator, La_2CuO_4 , to a metal of LSCO is continuous although there is a controversy as for the MIT.

III. CALCULATION OF THE EFFECTIVE MASS

For the metallic system regarded as a real synthetic metal with an electronic structure such as Fig. 1 (b), the effective mass of quasiparticles needs to be calculated. Hamiltonians of the metallic system can be considered as follows. Hamiltonian, H , is given by

$$H = H_1 + H_2, \quad (1)$$

$$H_1 = \sum_k (a_{k\uparrow}^\dagger a_{k\uparrow} + a_{k\downarrow}^\dagger a_{k\downarrow}) \epsilon_k + U \sum_g a_{g\uparrow}^\dagger a_{g\downarrow}^\dagger a_{g\downarrow} a_{g\uparrow}, \quad (2)$$

$$H_2 = - \sum_{i,j} E_p (Q_i - Q_j)^2, \quad (3)$$

where $a_{k\uparrow}^\dagger$ and $a_{g\uparrow}^\dagger$ are the creation operators for electrons in the Bloch state k and the Wannier state g , respectively, and ϵ_k is the kinetic energy when $U=0$. H_1 and H_2 are Hamiltonians of the metallic region C and the CDW-insulator regions B and D, respectively. In the case of Fig. 1 (a) and (c), the Hamiltonian is reduced to H_1 because H_2 disappears due to $\delta Q = 0$, and the on-site Coulomb energy is given by $U = \rho^2 U'$. H_1 is consistent with the Hamiltonian used in the Gutzwiller variational theory⁴.

In order to calculate the effective mass of quasiparticles and the ground-state energy for a strongly correlated metallic system, the Gutzwiller variational theory^{4,27-29} is used. H_1 is supposed to describe the metallic system. The wave function is written as

$$|\Psi\rangle = \eta^{\bar{\nu}} |\Psi_0\rangle, \quad (4)$$

where $|\Psi_0\rangle$ is the wave function when $U = 0$, $\bar{\nu}$ is the number of doubly occupied atoms, and $0 < \eta < 1$ is variation.⁴ The expectation value of H_1 is regarded to be

$$\langle H \rangle = \frac{\langle \Psi | \sum_{ij} \sum_{\sigma} t_{ij} a_{i\sigma}^{\dagger} a_{j\sigma} | \Psi \rangle + \langle \Psi | U \sum_i \rho_{i\uparrow} \rho_{i\downarrow} | \Psi \rangle}{\langle \Psi | \Psi \rangle}. \quad (5)$$

The second part of the equation is simply given by $\langle \Psi | U \sum_i \rho_{i\uparrow} \rho_{i\downarrow} | \Psi \rangle = U \bar{\nu}$ because $|\Psi_0\rangle$ is an eigenstate of the number operator $\sum_i \rho_{i\uparrow} \rho_{i\downarrow}$. The first part is dealt with by assuming that the motion of the up-spin electrons is essentially independent of the behavior of the down-spin particles (and *vice versa*). By minimization with respect to η , Gutzwiller obtained an extremely simple result for the ground-state energy, namely,

$$E_g/l = q_{\uparrow}(\bar{\nu}, \rho_{i\uparrow}, \rho_{i\downarrow}) \bar{\epsilon}_{\uparrow} + q_{\downarrow}(\bar{\nu}, \rho_{i\uparrow}, \rho_{i\downarrow}) \bar{\epsilon}_{\downarrow} + U \bar{\nu}. \quad (6)$$

Here,

$$\bar{\epsilon}_{\sigma} = l^{-1} \langle \Psi | \sum_{ij} t_{ij} a_{i\sigma}^{\dagger} a_{j\sigma} | \Psi \rangle = \sum_{k < k_F} \epsilon_k < 0 \quad (7)$$

is the average energy of the σ spins without correlation and ϵ_k is the kinetic energy in H_1 , with the zero of energy chosen so that $\sum_k \epsilon_k = 0$. $\bar{\epsilon}_{\uparrow}$ is equal to $\bar{\epsilon}_{\downarrow}$.

The discontinuities, q_{σ} , in the single-particle occupation number at the Fermi surface are given by

$$q_{\sigma} = \frac{\left(\sqrt{(\rho_{\sigma} - \bar{\nu})(1 - \rho_{\sigma} - \rho_{-\sigma} + \bar{\nu})} + \sqrt{(\rho_{-\sigma} - \bar{\nu})\bar{\nu}} \right)^2}{\rho_{\sigma}(1 - \rho_{\sigma})}, \quad (8)$$

where $\rho_{\sigma} = \frac{1}{2}\rho$, $0 < \rho \leq 1$ and $\rho_{\uparrow} = \rho_{\downarrow}$.^{27,28} This, calculated by Ogawa et. al.²⁷ who simplified the Gutzwiller variational theory, is in the context of the Gutzwiller variational theory. Eq. (8) is a function of ρ_{σ} and $\bar{\nu}$ irrespective of the quantity of charges. This can be analyzed in two cases of $\rho=1$ and $0 < \rho < 1$, because Gutzwiller did not limit the number of electrons on an atom for the metallic system.

In the case of $\rho=1$,

$$q_{\sigma} = 8\bar{\nu}(1 - 2\bar{\nu}). \quad (9)$$

This was described in the BR picture.

In the case of $0 < \rho < 1$, two kinds of q_{σ} can be considered. One is Eq. (8) when the electronic structure is $\delta Q \neq 0$, as shown in Fig. 1 (b). However, Eq. (8) can not be applied to the metallic system, as mentioned in the above section. The other is Eq. (9) when the electronic structure is $\delta Q=0$, as shown in Fig. 1 (c). Eq. (9) is obtained from substituting ρ_{σ} in Eq. (8) with ρ'_{σ} . Here, $\rho' = (n'/l) = 1$ and $\rho'_{\sigma} = \frac{1}{2}$, because the number of the effective charges, n' , is equal to l . It should be noted that the metallic system with less than one electron per atom, as shown in Fig. 1 (c), is mathematically consistent with that with one electron per atom, as shown in Fig. 1 (a).

Although the following calculations were performed by Brinkman and Rice,³ the calculations are applied to the effective mass. In the case of Fig. 1 (c), by applying Eq. (9) to Eq. (6) and by minimizing it with respect to $\bar{\nu}$, the number of the doubly occupied atoms is obtained as

$$\begin{aligned} \bar{\nu} &= \frac{1}{4} \left(1 + \frac{U}{8\bar{\epsilon}} \right) = \frac{1}{4} \left(1 - \frac{U}{U_c} \right), \\ &= \frac{1}{4} (1 - \kappa \rho^2), \end{aligned} \quad (10)$$

where $U_c = 8|\bar{\epsilon}|$ because of $\bar{\epsilon} = \bar{\epsilon}_{\uparrow} + \bar{\epsilon}_{\downarrow} < 0$, $U = \rho^2 U'$ and $U' = \kappa U_c$. $0 < \kappa \leq 1$ is the correlation strength. By applying Eq. (10) to Eq. (9) again, the effective mass is given by

$$\begin{aligned} q_{\sigma}^{-1} &= \frac{m^*}{m} = \frac{1}{1 - \left(\frac{U}{U_c}\right)^2}, \\ &= \frac{1}{1 - \kappa^2 \rho^4}. \end{aligned} \quad (11)$$

Although the separate conditions are $0 < \rho \leq 1$ and $0 < \kappa \leq 1$, m^* is defined under the combined condition $0 < \kappa \rho^2 < 1$ and is an average of the true effective mass in the BR picture for metal phase (region C in Fig. 1 (b)). The effective mass increases as it approaches $\kappa=1$ and $\rho=1$. For $\kappa \neq 0$ and $\rho \rightarrow 0$, the effective mass decreases and, finally, the metallic system undergoes a normal (or band-type) metal-insulator transition; this transition is continuous. The system at $\kappa \rho^2 = 1$ can be regarded as the insulating state which is the paramagnetic insulator because $\bar{\nu} = 0$. At a κ value (not one), the MIT from a metal at a ρ value of just below $\rho=1$ to the insulator at both $\rho=1$ and $\kappa=1$ is the first-order transition on band filling. This has been called the Mott transition by a lot of scientists including author. However, this is theoretically not the Mott transition which is an first-order transition from a value of U to U_c in a metal with the electronic structure of one electron per atom at $\rho=1$, as given in the BR picture. The Mott transition does not occur in real crystals because a perfect single-phase metal with $\rho=1$ is not made. Conversely, by hole doping (or electron doping to a metallic system with hole carriers) of a very low concentration, the first-order transition from the insulator with $\bar{\nu}=0$ to a metal can be interpreted as an abrupt breakdown of the balanced critical Coulomb interaction, U_c , between electrons. Then, the U_c value in the insulator reduces to a U value in a metal phase and an insulating phase produces due to doping of opposite charges, as shown in Fig. 1(d). This first-order transition with band filling is very important result found in this picture, which differs from the continuous (Mott-Hubbard or second-order) transition by a large U given by the Hubbard theory.

In order to obtain the expectation value of the energy in the (paramagnetic) ground state, Eqs. (10) and (11) are applied to Eq. (6). E_g is given by

$$E_g/l = \bar{\epsilon}(1 - \kappa \rho^2)^2. \quad (12)$$

As $U/U_c = \kappa\rho^2$ approaches one, E_g goes to zero.

In addition, the spin susceptibility in the BR picture is replaced by

$$\chi_s = \frac{m^*}{m} \frac{\mu_B^2 N(0)}{(1 - \frac{1}{2}N(0)\kappa\rho^2 U_c \frac{1+\frac{1}{2}\kappa\rho^2}{(1+\kappa\rho^2)^2})}, \quad (13)$$

where $N(0)$ is the density of states at the Fermi surface and μ_B is the Bohr magneton. The susceptibility is proportional to the effective mass which allows the enhancement of χ_s .

In the above picture, m^* , E_g/l and χ_s are the averages of true effective values in region C in Fig. 1 (b) which is described by the BR picture, and are justified only by means of measurement. The true effective ones in the BR picture are not measured experimentally, as mentioned in an above section. In particular, the magnitude of the true effective mass in the BR picture has the same value regardless of the extent of region C, while the measured effective mass depends upon the extent of region C.

IV. CONCLUSION

In order to evaluate true correlation strengths of $\text{Sr}_{1-x}\text{La}_x\text{TiO}_3$ and YBCO, explanations not given in the previous paper¹⁶ are appended. The experimental data of the heat capacity of $\text{Sr}_{1-x}\text{La}_x\text{TiO}_3$ was well fitted by Eq. (11) with $\kappa=1$ for all x below $x = \rho=0.95$. $\kappa=1$ indicates that the effective mass has a constant value although ρ changes. The increase of x to $x=0.95$ corresponds to the increase of region C. Because region C is described by the BR picture, the true correlation strength, $\kappa_{BR} = U/U_c$, of the BR picture can be found. When it is assumed that the extent of the metal phase (region C) at $x=0.95$ is closely the same as that at $\rho=1$, a value of $m^*/m = 1/(1 - \rho^4)$ at $x = \rho=0.95$ and $\kappa=1$ is approximately equal to that of $m^*/m = 1/(1 - \kappa_{BR}^2)$ in the BR picture. Then $\kappa_{BR} = (0.95)^2=0.90$ is obtained, which indicates that $\text{La}_{1-x}\text{Sr}_x\text{TiO}_3$ is very strongly correlated. Moreover, the decrease of the effective mass from $x=0.95$ to $x=0$ is the effect of measurement not the true effect.

In the case of $\text{YBCO}_{6+\rho}$ at $\rho=0.96$, as shown in Fig. 1 (c) and (d) of reference 16, the true correlation strength is determined as $\kappa_{BR}=0.92$ by the same above method. High- T_c superconductivity for YBCO is attributed to the true effective mass caused by the large κ_{BR} value. The heat capacity data measured by Loram et al.²⁴ seems to be explained by the above picture, too.

As another experimental result, the first-order transition at $x=0.02$ for $h\text{-BaNb}_x\text{Ti}_{1-x}\text{O}_3$ was observed, which may also be in the context of the above picture.³⁰ The validity of the BR picture is indirectly proved through the above picture. Furthermore, the combination of the above picture and the BR picture³ is called the extended BR picture defined in $0 < \kappa\rho^2 < 1$.

ACKNOWLEDGEMENTS

I would like to acknowledge Dr. Kwang-Yong Kang for providing the research environment necessary for this research.

* This was merged in a full-paper presented at NATO Advanced Research Workshop on New Trends in Superconductivity held at Yalta in Ukraine at Sept. 16-20 of 2001. Please see cond-mat/0110112.

** kimht45@hotmail.com.

** htkim@etri.re.kr..

¹ N. F. Mott, Metal-Insulator Transitions, Chapter 3, (Taylor & Frances, 2nd edition, 1990).

² J. Hubbard, (III) *ibid* **281**, (1965) 401.

³ W. F. Brinkman and T. M. Rice, *Phys. Rev.* **B2**, (1970) 4302.

⁴ M. C. Gutzwiller, *Phys. Rev.* **137**, (1965) A1726.

⁵ X. Y. Zhang, M. J. Rozenberg, and G. Kotliar, *Phys. Rev. Lett.* **70**, (1993) 1666.

⁶ A. Georges, G. Kotliar, W. Krauth, and M. J. Rozenberg, *Rev. Mod. Phys.* **68**, (1996) 13.

⁷ M. Imada, A. Fujimori, and Y. Tokura, *Rev. Mod. Phys.* **70**, (1998) 1039.

⁸ T. Moriya, BUTSURI (edited by Physical Society of Japan), Vol 54, No. 1, (1999) 48 (Japanese).

⁹ H. Fukuyama, M. Imada, and T. Moriya, BUTSURI (edited by Physical Society of Japan), Vol 54, No. 2, (1999) 123 (Japanese).

¹⁰ Y. Tokura, Y. Taguchi, Y. Okada, Y. Fujishima, T. Arima, K. Kumagai, and Y. Iye, *Phys. Rev. Lett.* **70**, (1993) 2126.

¹¹ K. Kumagai, T. Suzuki, Y. Taguchi, Y. Okada, Y. Fujishima, and Y. Tokura, *Phys. Rev. B* **48**, (1993) 7636.

¹² K. Morikawa, T. Mizokawa, K. Kobayashi, A. Fujimori, H. Eisaki, S. Uchida, F. Iga, and Y. Nishihara, *Phys. Rev. B* **52**, (1995) 13711.

¹³ I. H. Inoue, O. Goto, H. Makino, N. E. Hussey, and M. Ishikawa, *Phys. Rev. B* **58**, (1998) 4372.

¹⁴ H. Makino, I. H. Inoue, M. J. Rozenberg, I. Hase, Y. Aiura, and S. Onari, *Phys. Rev. B* **58**, (1998) 4384.

¹⁵ C. C. Tsuei, C. C. Chi, D. M. Newns, P. C. Pattnaik, and M. Daumling, *Phys. Rev. Lett.* **69**, (1992) 2134.

¹⁶ Hyun-Tak Kim, *Physica C* **341-348**, (2000) 259:cond-mat/0001008.

¹⁷ T. M. Rice and L. Sneddon, *Phys. Rev. Lett.* **47**, (1981) 689.

¹⁸ Hyun-Tak Kim, *Phys. Rev. B* **54**, (1996) 90.

¹⁹ T. Timusk and B. Statt, *Rep. Prog. Phys.* **62**, (1999) 61.

²⁰ S. H. Blanton, R. T. Collins, K. H. Kelleher, L. D. Rotter, Z. Schlesinger, D. G. Hinks, and Y. Zheng, *Phys. Rev. B* **47**, (1993) 996.

²¹ M. A. Karlow, S. L. Cooper, A. L. Kotz, M. V. Kelvin, P. D. Han, and D. A. Payne, *Phys. Rev. B* **48**, (1993) 6499.

²² Hyun-Tak Kim, H. Uwe, and H. Minami, *Advances in Superconductivity VI* (Springer-Verlag, Tokyo, 1994), P. 191.

²³ H. Ding, T. Yokaya, J. C. Campuzano, T. Takahashi, M. Randeria, M. R. Norman, T. Mochiku, K. Kadowaki, and

- J. Giapinzakis, *Nature* **382**, (1996) 51.
- ²⁴ J. W. Loram, K. A. Mirza, J. R. Cooper, W. Y. Liang, and J. M. Wade, *Journal of Superconductivity* **7**, (1994) 243.
- ²⁵ J. W. Loram, J. L. Luo, J. R. Cooper, W. Y. Liang, and J. L. Tallon, *Physica C* **341-348**, (2000) 831.
- ²⁶ A. Junod, D. Eckert, T. Graf, G. Triscone, and J. Muller, *Physica C* **162-164**, (1989) 482.
- ²⁷ Tohr Ogawa, Kunihiko Kanda, and Takeo Matsubara, *Prog. Theor. Phys.* **53**, (1975) 614.
- ²⁸ Dieter Vollhardt, *Rev. Mod. Phys.* **56**, (1984) 99.
- ²⁹ Patrick Fazekas, *Lecture Notes on Electron Correlation and Magnetism*, Chapter 9, (World Scientific Co., 1999).
- ³⁰ M. N. Khan, Hyun-Tak Kim, H. Minami, and H. Uwe, *Materials Letters* **47**, (2001) 95.

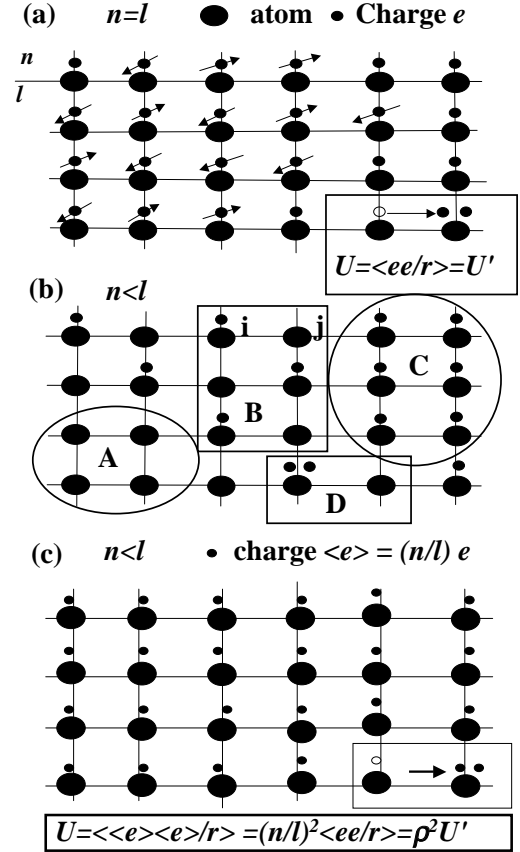


FIG. 1. (a) In the case of one electron per atom, the on-site Coulomb repulsion is given by $U = \langle \frac{e^2}{r} \rangle = U'$. (b) In the $n < l$ case, the four possible electronic structures are region A (insulator), region C (metal), and regions B and D (CDW insulator). Here, n corresponds to the number of carriers in region C. (c) The metallic structure in the case of less than one electron per atom is shown. $U = (n/l)^2 \langle \frac{e^2}{r} \rangle = \rho^2 U'$.